J Osaka Dent Univ 2021 (April) ; **55 (1)** : 99−111.

Biomechanical analysis of advance movement by bilateral sagittal split ramus osteotomy

***Yoshimi Morimoto[1], Tomokazu Motohashi[2] and Masahiro Nakajima[2]**

[1]Graduate School of Dentistry (Second Department of Oral and Maxillofacial Surgery) and [2]Second Department of Oral and Maxillofacial Surgery, Osaka Dental University, 8-1 Kuzuhahanazono-cho, Hirakata-shi, Osaka 573-1121, Japan

Sagittal split ramus osteotomy (SSRO) is widely used as an excellent surgical technique with a wide range of indications for jaw deformities. However, regression after advancement of the mandible is considered problematic compared with that after setback. We constructed models of 5- and 10-mm advancement after SSRO, and performed mechanical analysis of changes over time in stress loading employing the 3-dimensional finite element method. Models of the mandible were prepared after SSRO using titanium plates and screws as osteosynthesis material after 5- and 10-mm advancement of the distal bone fragment. Occlusal force and the muscular strength of the closing muscles were applied to each model. The displacement was greater in the 10-mm model than in the 5-mm model with conventional and locking screw fixation, whereas it was smaller in the model with locking plate fixation than in that with conventional plate fixation. In addition, it was smaller in the model with 2-plate fixation than in the one with 1-plate fixation. 2-plate fixation with locking screws may be a useful bone fragment fixation method because the amount of advancement increases, leading to postoperative stability. (J Osaka Dent Univ 2021 ; 55 : 99-111)

Key words : Sagittal split ramus osteotomy ; SSRO ; Three-dimensional finite element method ; 3D-FEM ; Biomechanical analysis

INTRODUCTION

Since Trauner and Obwegeser[1] reported sagittal split ramus osteotomy (SSRO) in 1957, many modified methods have been devised, such as the Obwegeser-Dal Pont method[2] and the Epker method.[3] It is now employed worldwide as a surgical procedure for jaw deformites such as mandibular prognathism, mandibular retrusion, open bite and mandibular asymmetry. Regression is a postoperative problem of SSRO and there are many reports on the optimal postoperative fixation method.[4-10] Favorable stability has been obtained by rigid fixation with bicortical screws to strongly secure bone fragments, and semi rigid fixation with miniplates applied after setback by SSRO has been reported.[11, 12] On the other hand, relapse after advancement of the mandible is considered problematic compared with that after setback.[13] However, few studies on the optimal fixation method for advancement by SSRO have been reported. We constructed models of 5- and 10-mm advancement after bilateral SSRO, performed mechanical analysis of time-course changes in stress loaded on the bone fragments, bone segment connection area, and bone plates employing the 3-dimensional finite element method (3-D FEM), and compared the models.

MATERIALS AND METHODS

Model of the mandible after SSRO

Using a computed tomography (CT) imaging apparatus (Bright Speed Elite Helical ; GE Healthcare, Chicago, IL, USA), we acquired maxillofacial images of healthy adult males using a tube voltage of 120 kV, tube current of 120 mA, and slice width of 0.625 mm. The CT data of 190 images of the mandibular condyle over the inferior border of the man-

dible were input into MECHANICAL FINDER version 10.0 (Research Center of Computational Mechanics, Tokyo, Japan). The bone contour line was extracted by thresholding in each CT image, detailed regions were corrected manually based on the CT images, and a 3D model of the mandible was prepared (Fig. 1 A). A material with a width of 2 mm was inserted between the proximal and distal bone segments at the time of sagittal split ramus osteotomy to construct a model consisting of the proximal bone segment, bone segment connection area, and distal bone segment after this osteotomy (Fig. 1 B). The osteotomy line was set according to the Obwegeser-Dal Pont method.[2] Mandibular models were prepared with 5-mm advancement (the 5-mm model) and 10-mm advancement (the 10-mm model) after SSRO (Fig. 1 C).

Then, using the Micro-Focusing CT imaging apparatus (inspeXio SMX-225 CT ; Shimadzu Corporation, Kyoto, Japan), CT images of the plate and screw (both from OsteoMed, Glendale, CA, USA) were acquired with a tube voltage of 160 kV, tube current of 40 mA, plate slice width of 0.038 mm, and screw slice width of 0.006 mm. The images were then converted to STL data (Figs. 1 D and E). The plate and screw presented as STL data were read into MECHANICAL FINDER version 10.0, and arranged in the mandibular models with 5- and 10-mm advancement after the sagittal split as follows. The plate and screw were placed on Champy's line in the model with 5- and 10-mm unilateral plates, as well as above and below Champy's line in the model with 2 unilateral plates to prepare models with monocortical fixation. The 5-mm advanced unilateral 1-plate model had 2,769,517 elements and 511,019 nodes (Fig. 2 A), the 10-mm advanced unilateral 1-plate model had 2,781,231 elements and 512,583 nodes (Fig. 2 B), the 5-mm advanced unilateral 2-plate model had 3,070,821 elements and 574,913 nodes (Fig. 2 C), and the 10-mm advanced unilateral 2-plate model had 3,100,496 elements and 579,643 nodes (Fig. 2 D). In each of the 4 models, plate fixation was done with conventional screws and locking screws. With the conventional screw fixation, the contact state was prepared by separating nodes in the contact region between the

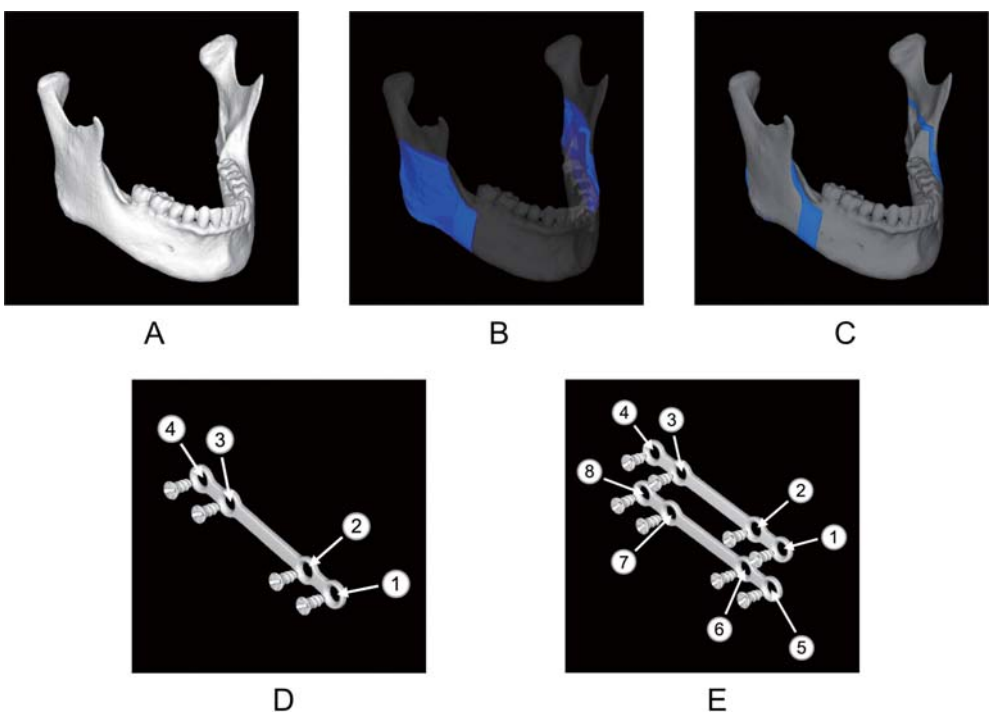

Fig. 1 Three-dimensional finite element model. (A) Mandible, (B) gap between advancement of the proximal and distal segments, (C) 3-FEM by sagittal splitting, (D) straight miniplate screws, and (E) ①-⑧ screw holes.

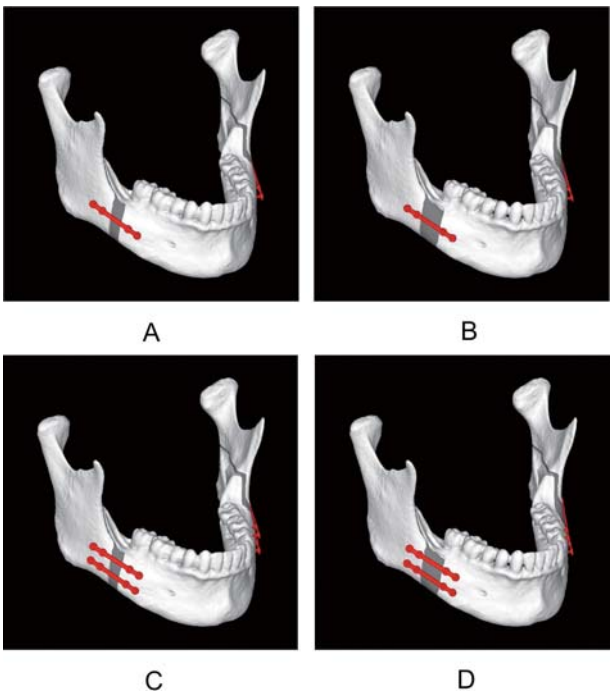

Fig. 2 Three-dimensional finite element model by SSRO. (A) Model of 5-mm advancement with 1-conventional plate or 1-locking plate, (B) model of 10-mm advancement with 1-conventional plate or 1-locking plate, (C) model of 5-mm advancement with 2-conventional plates or 2-locking plates, and (D) model of 10-mm advancement with 2-conventional plates or 2-locking plates.

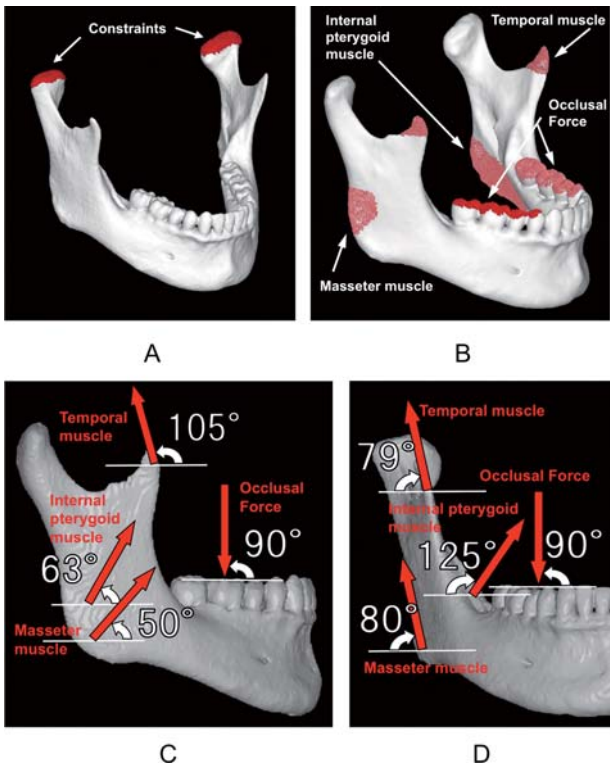

Fig. 3 Establishment of constraints and constraint loadings. (A) Constraints, (B) loads from the jaw closing muscles and occlusal force, and (C and D) loading directions and values.

plate and screw, while with locking screw fixation, the fixed state was prepared by sharing nodes in the contact region between the plate and screw.

Setting the physical properties of the proximal and distal segments

Young's modulus was converted from the CT Hounsfield unit using the relational expression reported by Carter *et al.*[14] for heterogeneous materials. Poisson's ratio was set at 0.4 according to the report from Van Buskirk *et al.*[15]

Physical properties of the gap between the proximal and distal segments

Physical properties of the gap between the proximal and distal segments were set according to the report by Okuda *et al.*[16] Young's modulus of the gap between the proximal and distal segments was set at 1, 3 and 6 months after surgery at 1.3787, 26.762 and 206.72 kgf/mm^2, respectively. The Young's modulus for 12 months was set to that of the normal mandible. Poisson's ratio was set at 0.4 according to the report from Van Buskirk *et al.*[15] The above values were set as the mandibular model for each postoperative period.

Material properties of the plates and screws

Based on the material properties of pure titanium, Young's modulus was set at 10,800 kgf/mm^2 and Poisson's ratio at 0.19.

Constraint and loading

Constraint

The bilateral condylar heads were completely constrained (Fig. 3 A).

Loading

Insertion

The jaw-closing muscles were set as follows based on the report from Kamijo.[17] Temporal muscle insertion was set at the coronoid process, masseter in-

sertion at the masseteric tuberosity on the mandibular angle, and internal pterygoid muscle insertion at the rough surface of the pterygoid muscle (Fig. 3 B).

Direction of action

The direction of action of each muscle was set as follows referring to the report from Yanagi *et al.*[18] From the center of insertion to the F-H plane, the temporal muscle was set at 105° posterosuperior, the masseter at 50° anterosuperior, and the internal pterygoid muscle at 63° anterosuperior. The temporal muscle was set at 79° superolateral to the sagittal plane, the masseter at 80° superolateral, and the internal pterygoid muscle at 125° superomedial (Figs. 3 C and D).

Strength of the jaw-closing muscles

The strength ratios of the the temporal muscle : masseter : internal pterygoid muscles were set at 6 : 3 : 1 according to the reports from Yanagi *et al.*[18] and Kojima *et al.,*[19] and the strength of each jaw-closing muscle was calculated to balance the vectors of occlusal force with the temporal, masseter, and internal pterygoid muscle strengths. The temporal muscle strength at 1, 3, 6 and 12 months after surgery was set at 22.08, 30.01, 34.78 and 39.68 kgf, respectively. The masseter muscle strength was set at 11.04, 15, 17.39 and 19.84 kgf, respectively. The internal pterygoid muscle strength was set at 3.67, 4.99, 5.78 and 6.6 kgf, respectively.

Occlusal force

A downward vertical load toward the occlusal plane was set in the bilateral molar regions. Referring to the report from Takashima *et al.,*[20] the occlusal force at 1, 3, 6 and 12 months after surgery was set at 20.79, 28.26, 32.75 and 37.38 kgf, respectively (Fig. 3 B).

Mechanical analysis

Analysis of stress on proximal and distal segments, and on the gap between the proximal and distal segments

The total equivalent stress on the proximal and distal segments, and on the gap between the proximal and distal segments during loading by the jaw-closing muscles and occlusal force were analyzed and compared.

Analysis of stress on the plates

The total equivalent stress on the plate, and the equivalent stress distributions in the center space of the plate and around screw holes ①-④ in the 1-plate model (Fig. 1 D) and the center space of the plate and around screw holes ①-⑧ in the 2-plate model (Fig. 1 E) were analyzed and compared.

Analysis of displacement of the distal segment

The displacement during loading was considered to be the distal segment displacement. This study was approved by the ethics committee of Osaka Dental University (Approval No.110975).

RESULTS

Equivalent stress in the proximal and distal segments (Table 1)

The total equivalent stress generated in the proximal segment slightly increased over time, although it slightly decreased at 6 months after surgery in both the 5- and 10-mm models with conventional and locking screw fixation. In addition, the total equivalent stress was greater in the 2-plate model than in the 1-plate model, and in the 10-mm model than in the 5-mm model throughout the experiment (Fig. 4). The total equivalent stress generated in the distal segment slightly increased over time in both the 5- and 10-mm models with conventional and locking screw fixation, and it was greater in the 2-plate model than in the 1-plate model throughout the experiment, whereas it was greater in the 10-mm model than in the 5-mm model until 6 months after surgery (Fig. 5).

Equivalent stress in the gap between the proximal and distal segments (Table 1)

The total equivalent stress generated in the gap between the proximal and distal segments was greater in the model with conventional screw fixation than in the one with locking screw fixation. In addition, the total equivalent stress was greater in the 10-mm model than in the 5-mm model throughout the experiment. Although it increased over time from 1 to 6 months after surgery, it decreased at 12

Table 1 Equivalent stress on the proximal segment, distal segment, gap between the proximal and distal segments, and miniplate.

		5-mm advancement by SSRO				10-mm advancement by SSRO			
		1 M	3 M	6 M	12 M	1 M	3 M	6 M	12 M
Proximal segment	1-conventional straight plate	319,289	359,008	353,912	423,713	341,624	368,999	359,231	427,687
	2-conventional straight plates	385,573	391,849	381,928	456,920	417,454	425,594	391,104	469,219
	1-locking straight plate	333,679	364,134	356,178	425,293	354,243	380,367	361,844	429,901
	2-locking straight plates	389,433	405,458	387,350	461,541	422,187	436,874	398,995	472,877
Distal segment	1-conventional straight plate	399,806	443,610	478,896	550,242	430,746	437,515	454,987	520,841
	2-conventional straight plates	440,937	478,673	518,715	596,345	450,795	478,334	498,530	570,798
	1-locking straight plate	399,090	442,665	477,072	548,240	422,198	441,449	454,207	519,304
	2-locking straight plates	425,561	477,613	514,249	590,714	441,580	483,042	495,743	566,972
Gap between the proximal and distal segments	1-conventional straight plate	12,716	39,688	115,282	89,074	16,818	60,538	152,067	132,455
	2-conventional straight plates	11,421	40,115	117,876	92,276	13,942	59,301	159,882	143,412
	1-locking straight plate	10,728	37,562	113,589	88,041	12,420	53,641	147,495	129,664
	2-locking straight plates	8,463	36,550	115,338	90,490	8,990	51,750	152,264	139,009
Miniplate	1-conventional straight plate	1,881,260	685,850	396,831	344,786	2,283,298	966,861	398,567	355,014
	2-conventional straight plates	2,451,513	1,040,695	559,176	563,815	3,336,426	1,397,980	584,074	545,072
	1-locking straight plate	3,041,740	1,141,541	576,816	541,534	3,646,215	1,586,541	650,293	573,020
	2-locking straight plates	3,438,510	1,544,311	842,036	811,334	4,007,707	2,087,903	872,431	809,984

(kgf/mm^2)

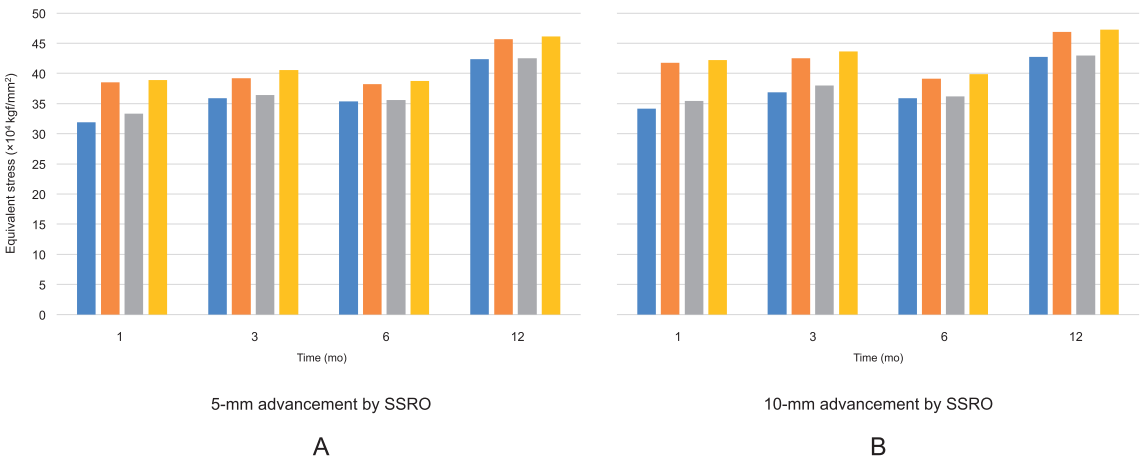

Fig. 4 Equivalent stress on the proximal segment with (A) 5-mm and (B) 10-mm advancement.
1-conventional straight plate, 2-conventional straight plates, 1-locking straight plate, 2-locking straight plates.

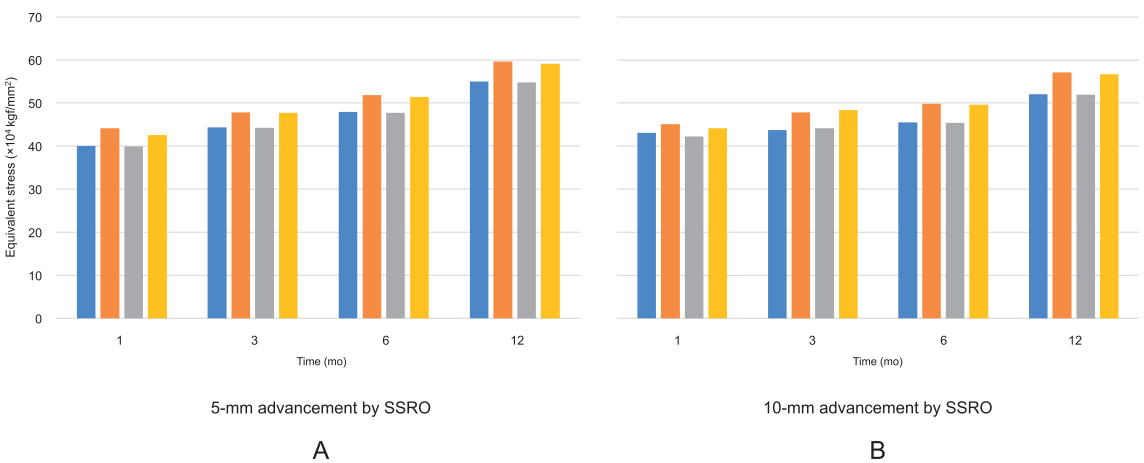

Fig. 5 Equivalent stress on the distal segment with (A) 5-mm and (B) 10-mm advancement.

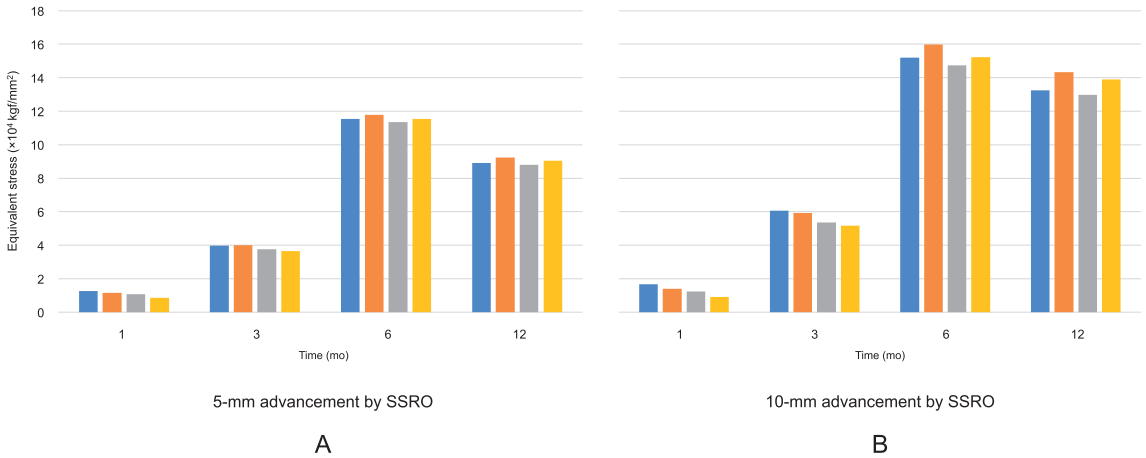

Fig. 6 Equivalent stress in the gap between the proximal and distal segments with (A) 5-mm and (B) 10-mm advancement.

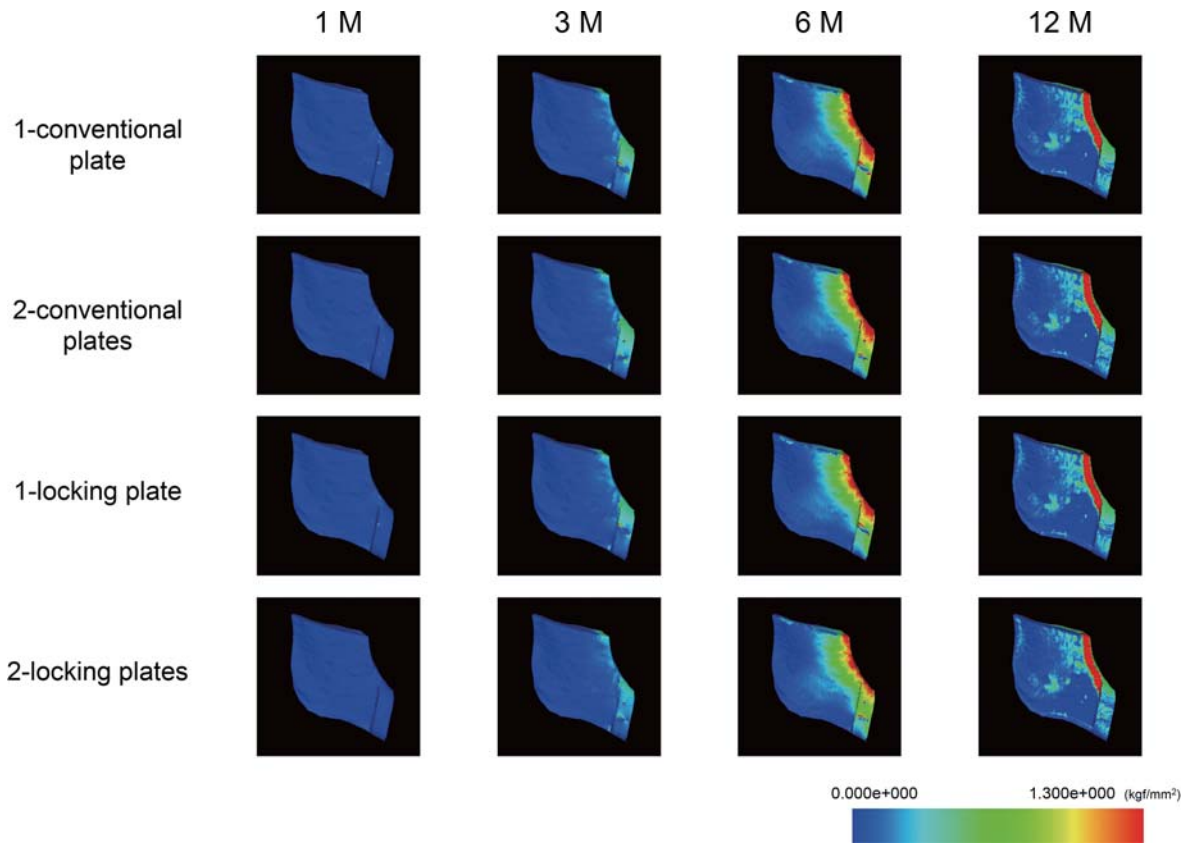

Fig. 7 Contours of equivalent stress in the gap between the proximal and distal segments with 5-mm advancement.

months (Fig. 6). The stress distribution was similar among all models, with the equivalent stress being concentrated in the anterior border of the mandibular ramus (Figs. 7 and 8).

Equivalent stress on the bone plate (Table 1)

The greatest total equivalent stress on the bone plate was noted 1 month after surgery in each model. Although it was greater in the 10-mm model than in the 5-mm model until 3 months after sur-

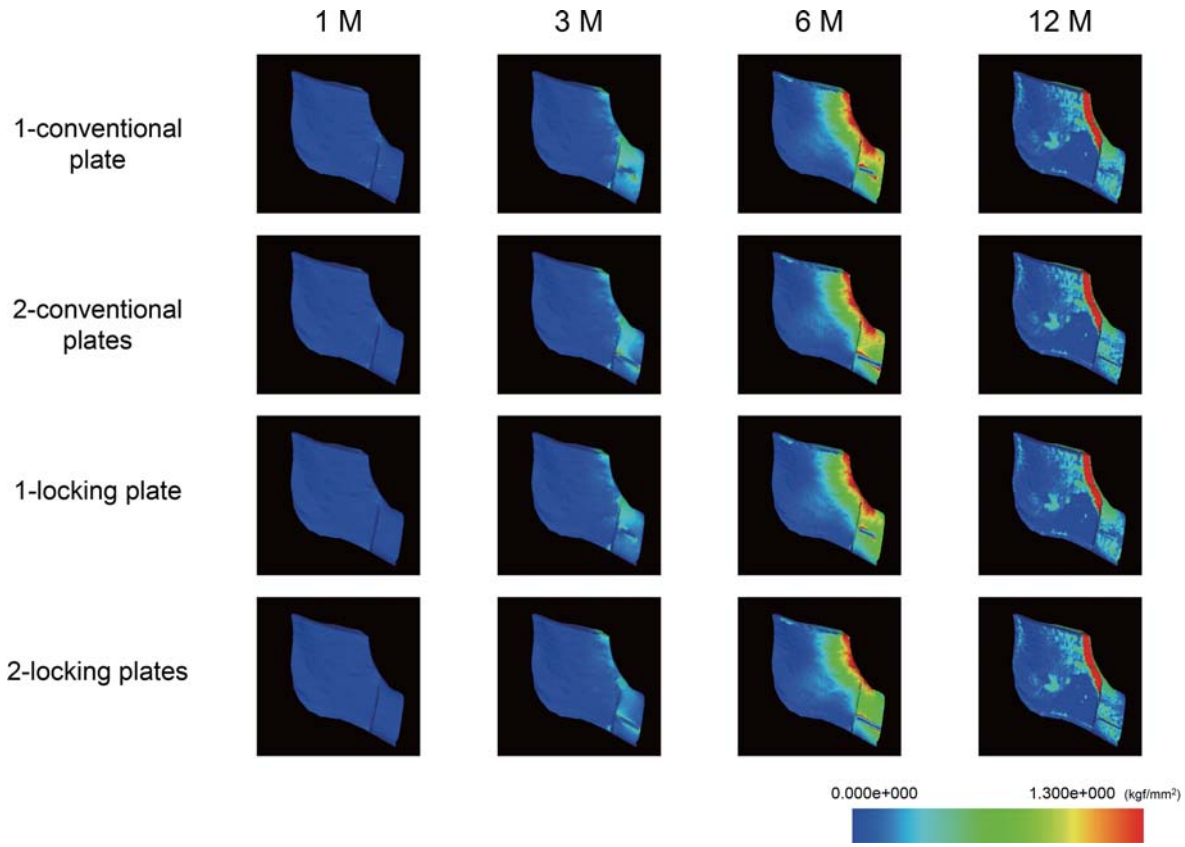

Fig. 8 Contours of equivalent stress in the gap between the proximal and distal segments with 10-mm advancement.

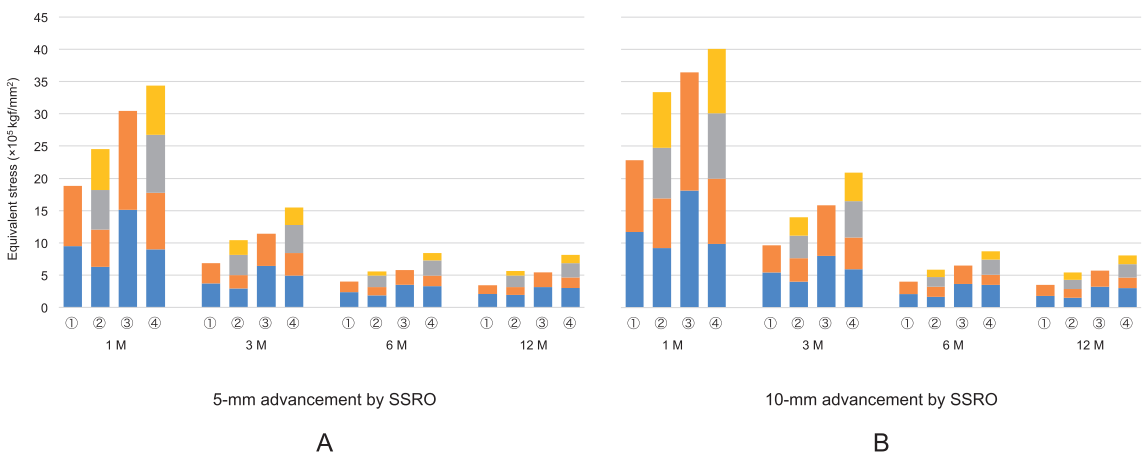

Fig. 9 Equivalent stress on both sides of miniplates with (A) 5-mm advancement and (B) 10-mm advancement.
① 1-conventional straight plate, ② 2-conventional straight plates, ③ 1-locking straight plate, ④ 2-locking straight plates,
Center right plate or upper right plate, Center left plate or upper left plate, Lower right plate, Lower left plate.

gery, almost no difference was noted at 6 and 12 months. The total equivalent stress was greater in the model with locking screw fixation than in the one with conventional screw fixation, and it was greater in the 2-plate model than in the 1-plate model. The total equivalent stress was the greatest in the 10-mm 2-plate model with locking screw fixation. On the other hand, in the models with 2-plate

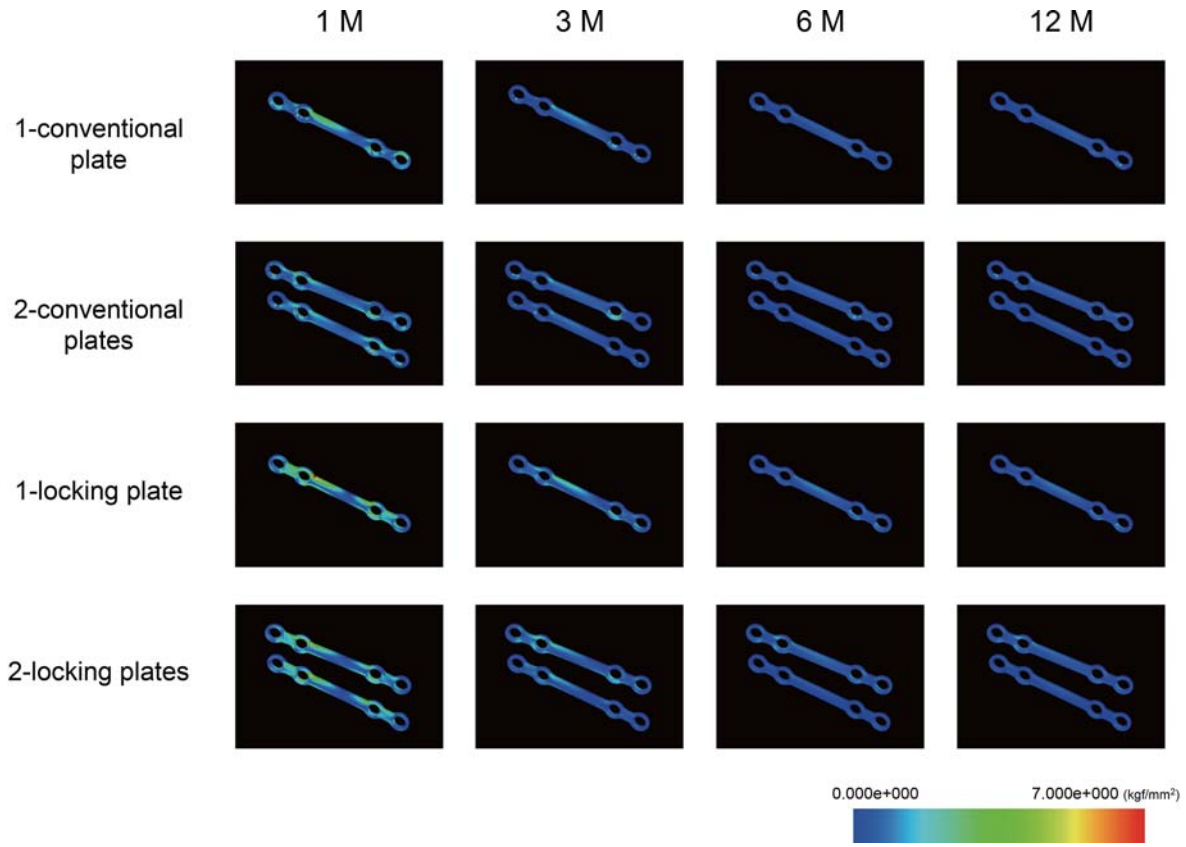

Fig. 10 Contours of equivalent stress on miniplates with 5-mm advancement.

fixation, the total equivalent stress generated on the respective plates was lower than that in the 1-plate model (Fig. 9). In the 1-plate model, stress was concentrated at the mesiodistal superior border of screw hole ③ and the mesial inferior border of ② over the distal inferior border of ③. In the 2-plate model, stress was concentrated at the distal superior border of screw hole ③ over the mesial superior border of ②, mesial inferior border of ② over the distal inferior border of ③, distal superior border of ⑦ over the mesial superior border of ⑥, and mesial inferior border of ⑥ over the distal inferior border of ⑦. The stress distribution was similar among all models (Figs. 10 and 11).

Displacement of distal segment

The displacement of the distal segment was the greatest at 1 month after surgery and then decreased over time. The displacement was greater in the 10-mm model than in the 5-mm model with conventional and locking screw fixation, whereas it was smaller in the model with locking plate fixation than in the one with conventional plate fixation, and it was smaller in the model with 2-plate fixation than in the one with 1-plate fixation (Fig. 12).

DISCUSSION

Rigid fixation with bicortical screws and semi rigid fixation with miniplates are now employed as an osteosynthesis method during orthognathic surgery at many facilities worldwide. In a questionnaire survey performed by the Japanese Society for Jaw Deformities, titanium plates, which are certain to acquire strong and reliable fixation, were most frequently used as a bone fragment fixation method for orthognathic surgery.[21] Stoelinga *et al.*[22] gave the following reasons for the use of miniplates : because fixation with miniplates does not require skin incision unlike bicortical screws and lag screws, the facial nerve will not be damaged ; the temporo-

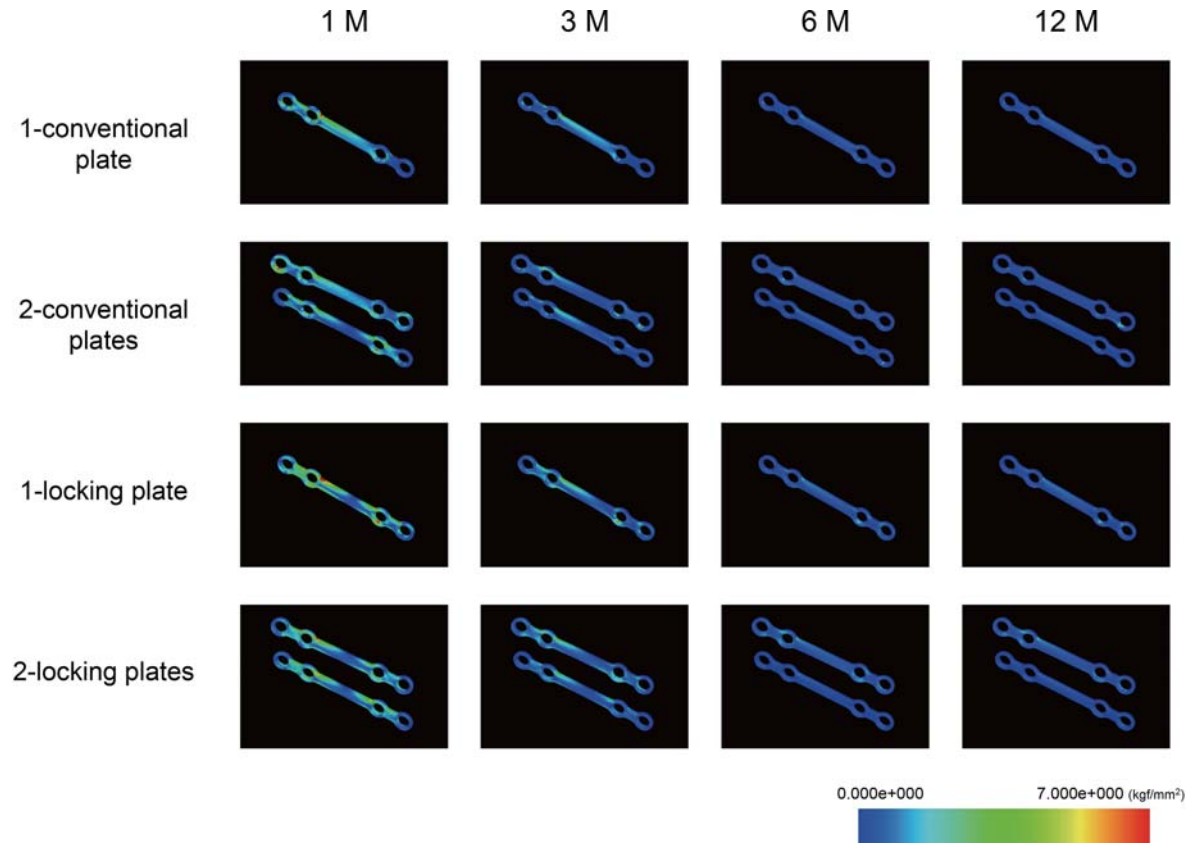

Fig. 11 Contours of equivalent stress on miniplates with 10-mm advancement.

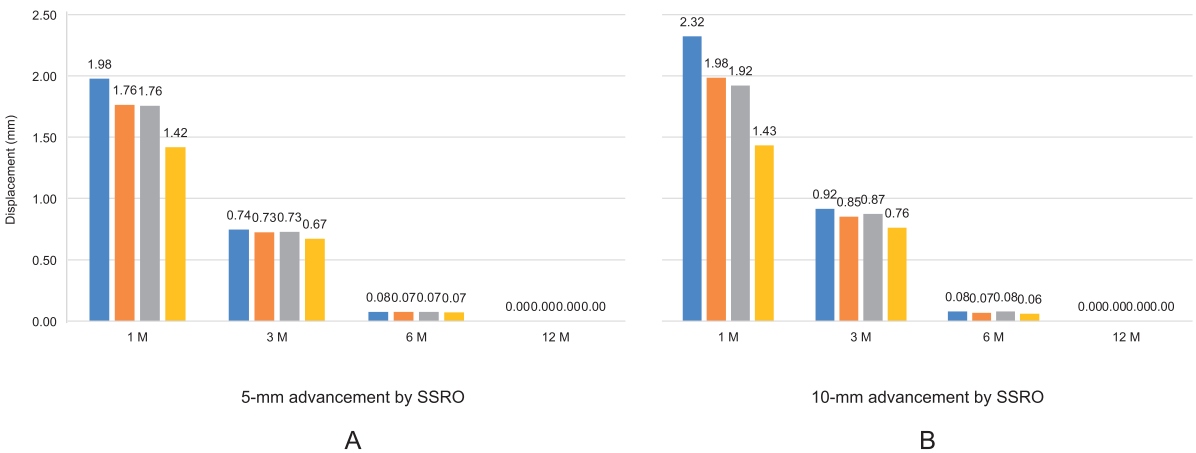

Fig. 12 Displacement in the distal segment with (A) 5-mm advancement and (B) 10-mm advancement.
1-conventional straight plate, 2-conventional straight plates, 1-locking straight plate, 2-locking straight plates.

mandibular joint is less affected ; there is no inferior alveolar nerve injury by the screws ; and positioning the distal segment is easy. We employed miniplate fixation for postoperative bone fragment fixation after SSRO. There have been many reports on stress analysis of bone fragment regions and the gap between the proximal and distal segments in plate orthognathic surgery employing different fixation methods. Mechanical investigations of bone fragment fixation using a polyurethane model were

done in many previous studies.[23-26] Studies using 3-D FEM have been reported recently.[27-30] It enables the analysis of osseous healing-induced changes in the occlusal force and physical properties of the gap between the proximal and distal segments accompanying recovery of the masticatory muscles over time. However, few studies have investigated the optimal method of fixation after advancement by SSRO. In this study, we prepared models in which the mandible was advanced by 5- or 10-mm, followed by conventional screw fixation or locking screw fixation with 1- or 2-miniplates, for 8 models in total, and performed time-course mechanical analysis at 1, 3, 6 and 12 months after surgery using 3-D FEM for comparison.

Equivalent stress on proximal and distal segments, and on the gap between the proximal and distal segments

The equivalent stress loaded on the proximal and distal segments slightly increased over time. However, it slightly decreased in the proximal segment at 6 months after surgery. This was due to transmission of the occlusal force and the stress of the strength of the jaw-closing muscles being increased by the osseous healing process in the gap between the proximal and distal segments. The stress transmission may have become similar to the physiological distribution at 12 months after surgery upon completion of osseous healing of this gap.

The equivalent stress on the gap between the proximal and distal segments increased from 1 to 6 months after surgery, and then decreased at 12 months. Rokutanda *et al.*[31] preformed postoperative time-course CT in patients who underwent SSRO or mandibular ramus vertical osteotomy, and compared the osseous healing process. They observed callus-like tissue 3 months after surgery. The gap between the bone fragments was filled with callus-like tissue at 6 months, and it became cortical bone -like tissue at 12 months. Bone remodeling from callus-like to cortical bone-like tissue continued from 6 to 12 months after surgery, suggesting that the equivalent stress loaded on the gap between the proximal and distal segments increased as the occlusal force recovered and dispersed upon completion of osseous healing, and resulted in the decrease at 12 months. In addition, stress was concentrated at the anterior border of the mandibular ramus in all models. Arakawa *et al.*[32] reported tensile stress at the anterior border of the mandibular ramus in the maximal intercuspal position during assessment of the mandibular stress distribution in subjects with normal occlusal force, suggesting that the stress of occlusal force and the strength of the jaw-closing muscles was transmitted to the gap between the proximal and distal segments.

Equivalent stress on the bone plate

The greatest equivalent stress loaded on the plate at the gap between the proximal and distal segments was noted 1 month after surgery, and then slightly decreased until 6 months. No difference was noted at 6 and 12 months. Nakajima *et al.*[33] and Tamura *et al.*[34] reported that plate fracture occurred within 3 months after surgery. In our study, the greatest stress was noted 1 month after surgery because osseous healing was not observed soon after surgery in the gap between the proximal and distal segments. This suggests that the stress on the gap between the proximal and distal segments decreases over time due to osseous healing of the gap. The stress at 12 months was not different from that at 6 months, even though the occlusal force and masticatory muscle strength increased upon completion of osseous healing. In addition, the stress was greater in the models with locking screw fixation than in those with conventional screw fixation.

Oguz *et al.*[35] compared stress between conventional titanium plate/screw fixation and locking plate /screw fixation after 5-mm advancement using 3-D FEM, and found that stress on the gap between the proximal and distal segments was greater with conventional titanium plate/screw fixation. Locking screws are known to be immobile because both the plate/screw and bone are fixed, which makes the connection among the plate, screw and bone complete and stable.[36] This suggests that strong and stable locking screw fixation dispersed stress gen-

erated in the gap between the proximal and distal segments across the plate. The total equivalent stress generated over the entire plate was greater in the 2-plate model than in the 1-plate model, and the greatest stress was noted in the 2-plate model with locking screw fixation. Takeshima *et al.*[37] applied 8 fixing methods to acrylic resin linear and U-shaped casts of a dried edentulous mandibular anterior molar region for comparison. They found that it was difficult to disperse stress by fixation with 1 plate alone, and found that there was a large displacement. In addition, the equivalent stress generated in each plate with 2-plate fixation was lower than that generated in the miniplate with 1-plate fixation.

Nakajima *et al.*[11] performed 3-D FEM of 1- and 2-miniplate fixation after setback of the mandible, and noted high stress at the anterior border of the mandibular ramus in 1-plate fixation. However, stress dispersion over the entire plate was noted with 2-plate fixation, although the stress was greater. This suggests that, among all models, the greatest stress observed after 10-mm advancement in the model with 2-plate locking screw fixation was due to the following mechanism. As the occlusal force and strength of the jaw-closing muscles act in different directions, torsion is generated between the proximal and distal segments. By using plates and locking screws in the 2-plate fixation, each plate is firmly fixed by the locking screws. Stress is dispersed in each plate because the stress generated in one plate is reduced. Choung *et al.*[38] prepared a 3-D FEM model of the stress of screw fixation after SSRO and suggested that the stress was most strongly concentrated at the superior border of the plate with a distal screw hole in the bone cutting line region, causing high torsional stress and bending stress concentrations within a narrow area on the screw surface in this region. This resulted in loosening of the screw. Similarly, in our study the greatest stress concentration was noted at the superior border of the plate with a distal screw hole in the lateral osteotomy region.

Displacement of the distal segment

The maximum displacement of the distal segment was noted in the 1-plate model with conventional screw fixation in both 5- and 10-mm advancement. In contrast, the minimum displacement was noted in the 2-plate model with locking screw fixation. Comparing the 5- and 10-mm advancement, the displacement differed between the 1- and 2-plate models with conventional screw fixation, and the 1-plate model with locking screw fixation. However, no difference was noted in the 2-plate model with locking screw fixation, suggesting that locking screw fixation in the 2-plate model is resistant to occlusal force and the strength of the jaw-closing muscles regardless of the amount of advancement because it is more strongly fixed. Therefore, favorable stability may be acquired by 2-plate fixation with locking screws as the amount of advancement increases.

Takano *et al.*[39] stated that strong bone fragment fixation is a factor for shortening of intermaxillary fixation. As excessive stress is generated by initiating jaw movement early after surgery to shorten the intermaxillary fixation, favorable fixation between the bone fragments may be important. When Okuda *et al.*[16] performed stress analysis of the miniplates and the gap between the proximal and distal segments in the healing process after mandible setback using 3-D FEM, they found that stress generated in the plate reached a maximum at 1 month after surgery and then decreased with osseous healing. Sigua-Rodriguez *et al.*[40] stated that 2-plate straight fixation may resist displacement after 10-mm advancement employing 3 fixing methods on stress analysis using 3-D FEM. Klein *et al.*[41] compared 6 fixing methods applied in a polyurethane model with 5- and 10-mm advancement, and reported that 2-plate straight fixation is the best for postoperative bone fragment fixation after SSRO accompanied by large advancement. They also found that the locking plate system is more resistant to masticatory muscle strength even if applied alone. Previously reported stress analysis was performed at only one time point after SSRO, whereas, we analyzed the stress at 1, 3, 6 and 12

months after advancement by SSRO. Locking screw fixation was stronger than conventional screw fixation in all models ; therefore, the equivalent stress generated in the intervening bone was small. Comparing the 5- and 10-mm advancement, the equivalent stress did not differ between the 2-plate models with locking screw fixation. As stress is dispersed in each plate, the stress generated in one plate is reduced. In addition, displacement of the distal segment is small. Therefore, the greater the advancement is, the more effective is the 2-plate fixation with locking screws. This is thought to contribute to the postoperative stability.

REFERENCES

1. Trauner R, Obwegeser H. The surgical correction of mandibular prognathism and retrognathia with consideration of genioplasty. I. Surgical procedures to correct mandibular prognathism and reshaping of the chin. *Oral Surgery Oral Med Oral Pathol* 1957 ; **10** : 677-689.
2. Dal Pont G. Retromolar osteotomy for the correction of prognathism. *J Oral Surg Anesth Hosp Dent Serv* 1961 ; **19** : 42-47.
3. Epker BN. Modifications in the sagittal osteotomy of the mandible. *J Oral Surg* 1977 ; **35** : 157-159.
4. Michiwaki Y. Long-term follow-up and relapse of the mandible after surgical correction (intraoral oblique sagittal splitting osteotomy) for mandibular prognathism. *J Jpn Stomatol Soc* 1989 ; **38** : 131-159. (Japanese)
5. Daimoto M, Sugawara J, Mitani H, Nagasaka H, Kawamura H. Postoperative stability of mandible and occlusion following intraoral vertical ramus osteotomy? : comparison with sagittal split ramus osteotomy with rigid fixation by titanium miniplate. *Jpn J Jaw Deform* 1997 ; **7** : 1120-128. (Japanese)
6. Hattori Y, Takagi R, Mutoh Y, Kaji M, Uchiyama N, Fukuda J, Ohashi Y, Hanada K. A follow-up study after orthognathic surgery for correction of mandibular prognathism with severe open bite —a comparison among kinds of osteosynthesis in sagittal split ramus osteotomy—. *Jpn J Jaw Deform* 1998 ; **8** : 186-191. (Japanese)
7. Kakizaki S, Kumazawa Y, Uchida M. Changes in mandible after sagittal splitting ramus osteotomy in mandibular prognathism —comparison of the circumferential wiring, screw and miniplate bone fixation methods—. *Odontology* 2000 ; **88** : 58-74. (Japanese)
8. Kawamoto T, Motohashi N, Hamada T, Imamura N, Fukada K, Nakagawa F, Ono T, Kato Y, Kuroda T. Dentofacial changes in seven patients treated by surgical advancement of the mandible. *Jpn J Jaw Deform* 2001 ; **11** : 182-193. (Japanese)
9. Kamiya N. Stability of mandible after sagittal split ramus osteotomy using difference fixation methods : a comparison between bi-cortical screw and mono-cortical locking plate methods. *Aichi-Gakuin J Dent Sci* 2014 ; **52** : 454-464. (Japanese)
10. Fujii H, Kuroyanagi N, Yamamoto S, Kamiya N, Miyachi H, Shimozato K. Stabilization of the proximal segment after sagittal split ramus osteotomy : two-dimensional plane analysis method made from superimposed three-dimensional computed tomography (3D-CT). *Aichi-Gakuin J Dent Sci* 2016 ; **54** : 419-428. (Japanese)
11. Nakajima M, Nakajima A, Shoju Y, Ozaki K, Dateoka S, Yamada K, Matsumoto K, Iseki T, Kakudo K. Biomechanical analysis of the occlusal force on osteosynthesis following sagittal split ramus osteotomy —comparison of one and two miniplate fixation—. *Shika Igaku*(*J Osaka Odontol Soc)* 2016 ; **79** : 1-9. (Japanese)
12. Tomita I, Tanaka S, Yasuda K, Furusawa K. Comparative study of postoperative evaluation by fixation methods in sagittal splitting ramus osteotomy. *J Matsumoto Dent Coll Soc* 2006 ; **32** : 199-204. (Japanese)
13. Kobayashi T, Kanoh H, Honma K, Shingaki S, Yamada K, Saito I, Hayashi T, Saito C. Temporomandibular joint symptoms and mandibular stability after orthognathic surgery in patients with mandibular retrognathism. *Jpn J Jaw Deform* 2002 ; **12** : 9-14. (Japanese)
14. Carter DR, Hayes WC. The compressive behavior of bone as a two-phase porous structure. *J Bone Joint Surg Am* 1977 ; **59** : 954-962.
15. Van Buskirk WC, Ashman RB. The elastic moduli of bone. *Trans Am Soc Mech Eng* 1981 ; **45** : 131-143.
16. Okuda K, Nakajima M, Kakudo K. Biomechanical analysis of the effect of occlusal force on osteosynthesis following sagittal split ramus osteotomy. *Shika Igaku*(*J Osaka Odontol Soc)* 2009 ; **72** : 9-17. (Japanese)
17. Kamijo Y. Oral anatomy. Tokyo : Anatom, 1966 : 252-261.
18. Yanagi T, Tsuji Y, Kishi M. The influence of location of occluding point and jaw elevator muscles forces on load of mandibular head. *J Tokyo Dent Coll Soc* 2001 ; **101** : 649-666. (Japanese)
19. Kojima T, Sato T. A morphological study of the tendon in human masticatory muscle. *Odontology* 1992 ; **80** : 342-366.
20. Takashima H, Ihara K, Noguchi N, Goto M, Katsuki T. Changes of masticatory function after sagittal splitting ramus osteotomy —from just before operation to one year after—. *Jpn J Jaw Deform* 1999 ; **9** : 157-166. (Japanese)
21. Katagiri W, Kobayashi T, Sasaki A, Susami T, Suda N, Tanaka E, Chikazu D, Tominaga K, Moriyama K, Yamashiro T, Saito I, Takahashi T. Investigation of surgical orthodontic treatment in Japan —a nation survey by Japanese society for jaw deformities in 2017—. *Jpn J Jaw Deform* 2020 ; **30** : 213-225. (Japanese)
22. Stoelinga PJW, Borstlap WA. The fixation of sagittal split osteotomies with miniplates : the versatility of a technique. *J Oral Maxillofac Surg* 2003 ; **61** : 1471-1476.
23. Uta S. Development of synthetic bone models for the evaluation of fracture fixation devices. *J Jpn Orthop Assoc* 1992 ; **66** : 1156-1164. (Japanese)
24. Muraji T, Suzuki S, Kuroda S, Yasui N, Imai K. Occlusal model in three-dimensional entity model. *Annual Report of Osaka Medical Association* 2002 ; **228** : 607-610. (Japanese)
25. Takahashi H, Furuta H, Moriyama S, Sakamoto Y, Matsunaga H, Kikuta T. Assessment of three bilateral sagittal split osteotomy techniques with respect to mandibular biomechanical stability by experimental study and finite element analysis simulation. *Med Bull Fukuoka Univ* 2009 ; **36** : 181-192.

26. Yamada M, Yamaji T. Evaluation of the fixation force by different type locking screw and different bone strength. *J Jpn Soc Fract Repair* 2019 ; **41** : 1140-1144. (Japanese)
27. Tanaka C, Arakawa T, Shinohara T, Katada H, Yamaguchi H. Analysis by 3-dimensional finite element method of mandibular lateral shift. *J Tokyo Dent Coll Soc* 2003 ; **103** : 169-180. (Japanese)
28. Bohluli B, Motamedi MHK, Bohluli P, Sarkarat F, Moharamnejad N, Tabrizi MHS. Biomechanical stress distribution on fixation screws used in bilateral sagittal split ramus osteotomy : assessment of 9 methods *via* finite element method. *J Oral Maxillofac Surg* 2010 ; **68** : 2765-2769.
29. Sindel A, Demiralp S, Colok G. Evaluation of different screw fixation techniques and screw diameters in sagittal split ramus osteotomy : finite element analysis method. *J Oral Rehabil* 2014 ; **41** : 683-691.
30. Motohashi T, Morimto Y, Shoju Y, Hamada H, Kubo H, Onishi Y, Tsunokuma M, Nakajima M. Biomechanical analysis by the three-dimensional finite element method of stress after sagittal split ramus osteotomy : comparison of titanium and u-HA/PLLA miniplate osteosynthesis. *Shika Igaku* (*J Osaka Odontol Soc)* 2018 ; **81** : 65-73. (Japanese)
31. Rokutanda S, Yamada S, Yanamoto S, Kawakita A, Fujimura Y, Morita Y, Rokutanda H, Yoshida N, Umeda M. Comparison of osseous healing process in the SSRO and IVRO : a preliminary study. *Jpn J Oral Diag* 2017 ; **30** : 157-167. (Japanese)
32. Arakawa T. Dynamic examination of the effect of unilateral biting on the mandible —analysis by means of the three-dimensional finite-element method—. *J Tokyo Dent Coll Soc* 1998 ; **98** : 685-703. (Japanese)
33. Nakajima M, Motohashi T, Okuda K, Sunada N, Shojyu Y, Yoshimoto H, Tanaka K, Kakudo K, Matsumoto N, Matsumoto T. Biomechanical analysis by the three-dimensional finite element method of stress in bone fixation plates after sagittal spliting ramus osteotomy. *J Osaka Dent Univ* 2007 ; **41** : 89-96.
34. Tamura N, Takaki T, Takano N, Shibahara T. Three-dimensional finite element analysis of bone fixation in bilateral sagittal split ramus osteotomy using individual models. *Bull Tokyo Dent Coll* 2018 ; **59** : 67-78.
35. Oguz Y, Uckan S, Ozden AU, Uckan E, Eser A. Stability of locking and conventional 2.0-mm miniplate/screw systems after sagittal split ramus osteotomy : finite element analysis. *Oral Surg Oral Med Oral Pathol Oral Radiol Endod* 2009 ; **108** : 174-177.
36. Shimozato K. Principles of internal fixation of the craniomaxillofacial skeleton : trauma and orthognathic surgery. Tokyo : Igaku-Shoin, 2017 : 54-55.
37. Takeshima H. Assessment of structural mechanics of osteosynthesis with titanium miniplates. *Jpn J Oral Maxillofac Surg* 1992 ; **38** : 849-862. (Japanese)
38. Chuong CJ, Borotikar B, Schwartz-Dabney C, Sinn DP. Mechanical characteristics of the mandible after bilateral sagittal split ramus osteotomy : comparing 2 different fixation techniques. *J Oral Maxillofac Surg* 2005 ; **63** : 68-76.
39. Takano M. Aiming to shorten the intermaxillary fixation period. *JOP* 2010 ; **26** : 30-34. (Japanese)
40. Sigua-Rodriguez EA, Caldas RA, Goulart DR, Hemerson de Moraes P, Olate S, Ricardo Barão VA, Ricardo de Albergaria-Barbosa J. Comparative evaluation of different fixation techniques for sagittal split ramus osteotomy in 10 mm advancements. Part two : Finite element analysis. *J Craniomaxillofac Surg* 2019 ; **47** : 1015-1019.
41. Klein GBG, Mendes GCB, Ribeiro Junior PD, Viswanath A, Papageorge M. Biomechanical evaluation of different osteosynthesis methods after mandibular sagittal split osteotomy in major advancements. *Int J Oral Maxillofac Surg* 2017 ; **46** : 1387-1393.